TAR-RNA recognition by a novel cyclic aminoglycoside analogue

Devanathan Raghunathan, Víctor M. Sánchez-Pedregal, Jochen Junker, Claudia Schwiegk, Markus Kalesse[1], Andreas Kirschning[1] and Teresa Carlomagno*

Department of NMR-based Structural Biology, The Max Planck Institute for Biophysical Chemistry, Am Fassberg, 11 D-37077 Göttingen, Germany and [1]Institute of Organic Chemistry, University of Hannover, Schneiderberg 1B, D-30167 Hannover, Germany

ABSTRACT

The formation of the Tat-protein/TAR-RNA complex is a crucial step in the regulation of human immunodeficiency virus (HIV)-gene expression. To obtain full-length viral transcripts the Tat/TAR complex has to recruit the positive transcription elongation factor complex (P-EFTb), which interacts with TAR through its cyclin T1 (CycT1) component. Mutational studies identified the TAR hexanucleotide loop as a crucial region for contacting CycT1. Interfering with the interaction between the Tat/CycT1 complex and the TAR-RNA is an attractive strategy for the design of anti-HIV drugs. Positively charged molecules, like aminoglycosides or peptidomimetics, bind the TAR-RNA, disrupting the Tat/TAR complex. Here, we investigate the complex between the HIV-2 TAR-RNA and a neooligoaminodeoxysaccharide by NMR spectroscopy. In contrast to other aminoglycosides, this novel aminoglycoside analogue contacts simultaneously the bulge residues required for Tat binding and the A35 residue of the hexanucleotide loop. Upon complex formation, the loop region undergoes profound conformational changes. The novel binding mode, together with the easy accessibility of derivatives for the neooligoaminodeoxysaccharide, could open the way to the design of a new class of TAR-RNA binders, which simultaneously inhibit the formation of both the Tat/TAR binary complex and the Tat/TAR/CycT1 ternary complex by obstructing both the bulge and loop regions of the RNA.

INTRODUCTION

Following the discovery that RNA plays a major role in several cellular functions, as for example transcriptional control and catalysis, a great deal of biochemical and structural research has been initiated around RNA, including its identification as a potential target for anti-viral therapy. The *trans*-activating region (TAR) RNA of the human immunodeficiency virus (HIV) is a particularly attractive example of the RNA-based drug discovery process. The formation of full-length viral transcripts requires the interaction of the TAR-RNA with the transcription activator protein, Tat (1). The Tat/TAR complex recruits the positive transcription elongation factor complex (P-EFTb), which activates the RNA polymerase II stalled at the TAR-RNA site and enables viral replication (2,3). The loop region of the TAR-RNA plays a key role in binding the CycT1 unit of the P-EFTb complex (4). Disruption of the Tat/TAR interaction inhibits the production of complete viral transcripts, as the P-EFTb complex cannot bind the TAR-RNA in the absence of the Tat-protein (2). Thus, the interaction of the TAR-RNA with both the Tat-protein and the P-EFTb complex represents an appealing target for anti-viral therapy.

The TAR-RNAs from HIV-1 and HIV-2 differ in the size of the bulge, which comprises 3 nt (UCU) in the HIV-1 and 2 nt (UU) in the HIV-2 (Figure 1B). Both TAR-RNAs recognize the Tat-protein in a similar manner. Of critical importance is the U23 nucleotide in the TAR bulge and the (G26–C39) and the (A27–U38) base pairs in the upper stem (Figure 1B) (5–7).

Given the relevance of the TAR-RNA as a potential therapeutic target, much work has been directed towards the synthesis and screening of small organic compounds that selectively bind to the TAR-RNA, thereby inhibiting the formation of the Tat/TAR complex. As a result of these

*To whom correspondence should be addressed. Tel: +49 551 201 2214; Fax: +49 551 201 2202; Email: taco@nmr.mpibpc.mpg.de
Present address:
Víctor M. Sánchez-Pedregal, Universidad de Santiago de Compostela, Facultad de Química, Departmento Química Orgánica, Campus Universitario Sur, s/n Postcode E-15782 Santiago de Compostela, Spain

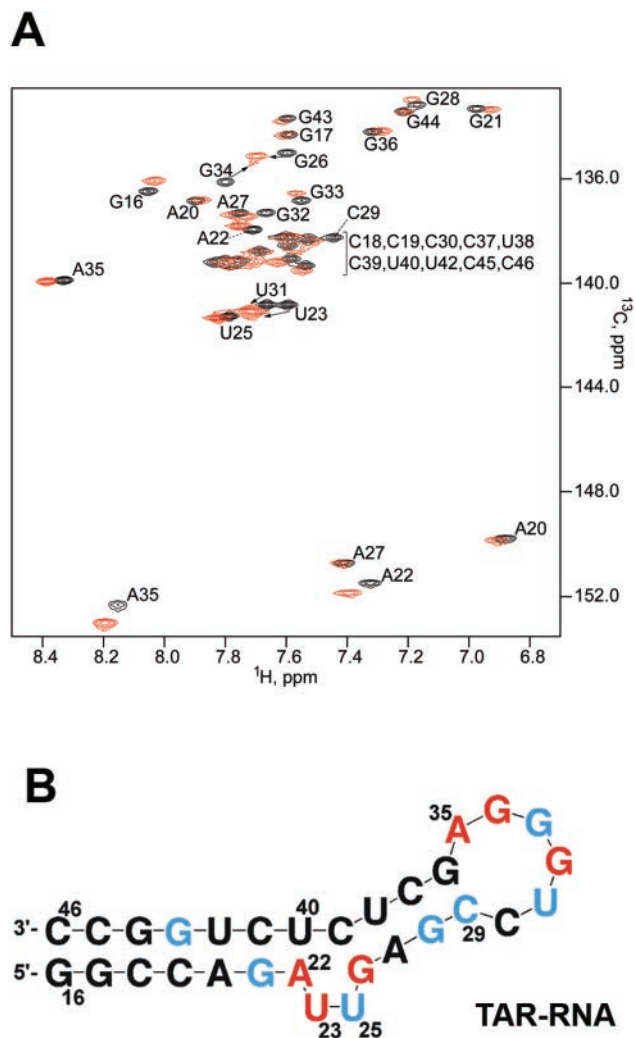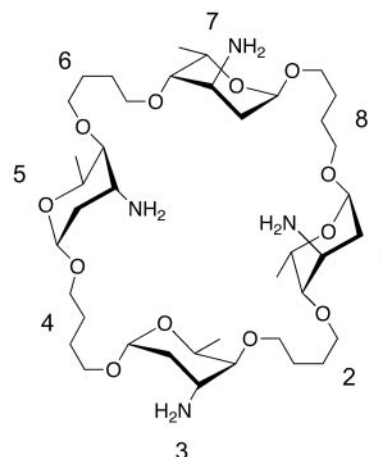**Scheme 1.** Aminoglycoside analogue **1**. Sugar and linker units are numbered clockwise from 1 to 8.

Figure 1. Chemical shift mapping of TAR-binding sites. (**A**) Superposition of the base region of a C–H correlation for the HIV-2 TAR-RNA free (black) and in complex with the aminoglycoside analogue **1** (red). The acquisition dimensions were 128 points (^{13}C) and 2048 points (^{1}H); each spectrum was acquired for a total of 5 h on a 600 MHz Bruker AVANCE spectrometer. (**B**) Sequence of the TAR-RNA. The lower stem of the free TAR-RNA comprises the base pairs from G16–C46 to A22–U40, while the upper stem comprises the base pairs from G26–C39 to C29–G36. The most significant chemical shifts changes upon binding of the TAR-RNA to **1** are observed either for the base or for the ribose C and H resonances of A22, U23, G26, G32, G34 and A35 (rendered in red). Less prominent chemical shift changes are observed for G21, U25, G28, C29, U31, G33, G36 and G43 (rendered in light blue).

studies, a number of small molecules have been found to interact with the TAR-RNA inhibiting viral transcription in HeLa cells (8–10).

The cationic antibiotics of the aminoglycoside family bind to several RNA motifs by specifically recognizing their 3D structure (11). In particular, they have been proven to exert an inhibitory effect on the binding of the Tat-protein to the TAR-RNA (12–14). The structure of the TAR-RNA in complex with neomycin B has been investigated by NMR (15): neomycin B binds the TAR-RNA in the minor groove of the lower stem, which results in an allosteric inhibition of Tat binding to TAR caused by a reduction of the major groove volume in the upper stem.

Aminoglycosides are valuable instruments to study the structural basis of RNA recognition and inhibition of function by cationic organic molecules. However, their use as RNA-targeting drugs is impeded by several drawbacks, such as low specificity, high toxicity and development of resistance (16–18). These considerations underline the continuous need for new compounds that share an aminoglycosidic scaffold but can be easily derivatized to obtain drug leads with a better pharmacological profile.

Here we present the structure of the HIV-2 TAR-RNA bound to a cyclic neooligoaminodeoxysaccharide (Scheme 1). The synthesis of this compound has been reported previously (19). This class of aminoglycoside analogues is unique in the fact that they are easily synthesized via metathesis olefination and provide novel methods of derivatization and functional group modification. The structural analysis conducted here reveals attractive features in the interaction of this ligand with the TAR-RNA. The aminoglycoside analogue **1** binds to two sites of the TAR-RNA: (i) the bulge and loop regions on the major groove side of the upper stem; and (ii) the minor groove of the lower stem. In contrast to natural aminoglycosides and like argininamide, **1** binds to the crucial residues of the TAR bulge required for Tat binding. Additionally, **1** extensively contacts the A35 residue of the dynamic hexanucleotide loop. Upon binding of **1** to A35, the loop becomes more ordered. Such structural stabilization could represent a general mechanism by which the Tat protein pre-orders the loop of the TAR-RNA for the binding of the P-TEFb complex. Thus, the simultaneous targeting of both the bulge and the loop of the TAR-RNA by positively charged molecules could result in a more efficient inhibition of the binding of both the Tat-protein and the P-TEFb complex to the TAR-RNA.

MATERIALS AND METHODS

Sample preparation

The TAR-RNA was obtained by *in vitro* transcription using T7-polymerase expressed and purified in-house. ^{15}N/^{13}C-labeled NTPs were purchased from Spectra Stable Isotopes.

The RNA was purified by gel electrophoresis. An aliquot of 20 ml transcription reaction yielded ∼5 mg of pure RNA. The aminoglycoside analogue **1** was obtained by chemical synthesis as described before (19).

NMR spectroscopy

NMR spectra were acquired using a 0.3 mM sample of $^{13}C/^{15}N$-labeled HIV-2 TAR-RNA dissolved in either D_2O or H_2O/D_2O (90/10%), containing 50 mM phosphate buffer at pH 6.4. Compound **1** was titrated in concentrations varying from 0.3 to 30 mM. The chemical shift changes of the resonances of both the base C5/C6/C8/H5/H6/H8 and the sugar $C1'/H1'$ atoms of the RNA were monitored in HSQC spectra (20) during the titration. Standard NMR methods were employed to assign the TAR-RNA in the complex (see also Supplementary Data) (3,21).

Intermolecular NOEs from the TAR-RNA to the ligand were assigned from a 3D ^{13}C-edited/^{12}C-filtered HSQC-NOESY spectrum in D_2O with a mixing time of 200 ms (22), where the NOEs between the ^{13}C-labeled RNA and the unlabeled aminoglycoside could be selectively observed. The aminoglycoside being in fast exchange between the free and bound forms, no intramolecular NOE restraints could be derived for the aminoglycoside in the complex. RNA intramolecular NOEs were derived from a 3D ^{13}C-HSQC-NOESY and from a base-selective high-resolution 3D ^{13}C-HSQC-NOESY (23) with mixing time of 100 ms.

The sugar pucker was defined as either $C2'$-*endo* or $C3'$-*endo* depending on the J coupling constants between $H1'$ and $H2'$ derived from a 2D-HCCH-E.COSY spectrum (24).

^{15}N-labeled aminoglycoside (25) was mixed with unlabeled TAR-RNA to attempt the measurement of H-bond mediated J_{NP} couplings to confirm or exclude the presence of hydrogen bonding between the amino groups of the aminoglycoside and the phosphate backbone of the RNA. The J-quantitative method (26) was used to measure the J_{NP} couplings in an H–N 2D correlation. The ^{15}N chemical shift of the amino group confirmed that all four groups of **1** are protonated in the NMR buffer. The resonances of the amino protons of **1** could not be observed due to fast exchange with the solvent.

T_1 relaxation times of the base C8/C6 carbons were measured in ^{13}C-^1H correlations using relaxation delays of 5, 10, 20, 30, 40, 60, 80, 100, 120, 160, 200, 300, 400, 600, 800 and 1200 ms.

The simultaneous presence of the negatively charged RNA and an excess of the positively charged ligand deterred us from using phages or bicelles to attempt the alignment of the RNA/ligand complex. Instead, we measured field-induced residual dipolar couplings (*fi*RDC) (27), which linearly scale with the square of the field strength. We measured the ^1H-^{13}C splitting (J + D) of the C2H2, C6H6, C8H8 and $C1'H1'$ at 600, 700 and 800 MHz. The dipolar couplings at 800 MHz were derived by linear fitting of the three values and extrapolation to zero magnetic field to obtain the value of J. In the refinement procedure we employed only those RDCs that showed a linear relationship to B_0^2 within the experimentally determined error limits (37 RDCs in total, excluding the two-base bulge, the loop and the two terminal residues).

Structure calculation

Restrained molecular dynamics (rMD) combined with energy minimization in XPLOR-NIH (28) was employed to obtain the final ensemble of structures of the TAR/neooligo-aminodeoxysaccharide complex. The restraints used in the calculations comprised a total of 447 NOEs for the RNA (320 intranucleotide and 127 internucleotide NOEs), 55 intermolecular NOEs, 44 experimental dihedral angle restraints defining the ribose pucker for 22 nt, 41 non-experimental dihedral angle restraints defining the backbone angles α, β, ζ and ε in the lower stem, 72 H-bond restraints defining 10 bp for stretches 16–21, 41–46 and 26–29, 36–39 and 10 restraints defining the planarity of the base pairs (Supplementary Data).

Chemical shift mapping and intermolecular NOEs identified three regions for the binding of the aminoglycoside analogue **1** on the TAR-RNA: the bulge and loop regions on the side of the upper stem major groove and the minor groove of the lower stem (Figure 1). As the contacts between the aminoglycoside analog **1** and the upper stem, bulge and loop of the TAR-RNA are much more extensive than those with the second binding site in the lower stem minor groove, a first round of structure calculations focused on the intermolecular recognition in the upper stem binding site only. The exact procedure used to assign the intermolecular NOEs to each of the four degenerate sugar and linker units of **1** is described in Supplementary Data.

A total of 150 structures were subjected to rMD. The protocol is described in detail in Supplementary Data. The 50 structures with lowest energy were subjected to a final refinement with the incorporation of the *fi*RDCs to validate the shape of the complex. In this final refinement protocol, the attractive Lennard-Jones potential term was switched on. The force constant for the dipolar coupling energy term was 1.5 kcal mol^{-1} Hz^{-2}. An accurate estimate of the magnitude D_{zz} and rhombicity R of the alignment tensor cannot be obtained from the powder pattern if only C–H dipolar couplings for the base and $C1'$-$H1'$ ribose vectors are available. Hence we performed a grid search where we evaluated the dipolar coupling energy term as a function of the alignment tensor. A systematic grid search for the optimal values of D_{zz} and R was performed by sampling values of D_{zz} between 5 and 10 in 1 Hz steps and values of R between 0.1 and 0.65 in 0.05 steps. Examination of the dipolar coupling energy profiles revealed a minimum for $D_{zz} = 7$ Hz and $R = 0.55$. Thus, this tensor was employed in the refinement (29). The correlation coefficients of the experimentally determined *fi*RDCs versus the calculated *fi*RDCs and the Q factors of the final structures were calculated using Dipo-Coup (30). The final structures were viewed and analyzed using MolMol (31).

The contacts of the aminoglycoside analog **1** with the lower stem minor groove are defined by the intermolecular NOEs of **1** with $G43$-$H1'$ and $G44$-$H4'$. Owing to steric reasons, these NOEs were assigned to the same sugar and linker units of **1**.

Both the RDCs and the relaxation data indicate that the TAR/**1** complex dimerizes. The procedure used for the definition of the dimer geometry and stoichiometry is explained in Results and in Supplementary Data. Briefly, the experimental

data are exclusively compatible with dimerization through one molecule of **1** bridging the lower stems of two molecules of TAR. Therefore, an additional molecule of **1** was docked to the minor groove of two TAR/**1** molecules, predisposed by rigid body dynamics in the correct orientation to satisfy the dimer geometry defined by the dipolar coupling data. The docking was performed by MD simulation in explicit water solvent and was guided by the NOEs of **1** to G43-H1′ and G44-H4′.

RNase footprinting

5′-^{32}P labeled HIV-2 TAR-RNA (Scheme 1) was digested with either RNase T1 (G-selective) or RNase A (selective for U and C) in the presence of the aminoglycoside analogue **1** at 4°C. The concentration of RNA was 10 μM, while the concentration of compound **1** varied from 0.1 μM to 10 mM. All experiments were performed in autoclaved Eppendorf reaction vessels. Extreme precaution was taken to avoid RNase contamination. After the reaction, the mixture was loaded onto a 20% denaturing polyacrylamide gel for analysis.

PACE experiment

The stoichiometry of the binding of the TAR-RNA to **1** was verified using the PACE technique (32). A series of lanes containing different concentrations of the aminoglycoside (0, 1, 2, 5, 7, 10, 20, 70, 100, 200 and 500 μM) were poured with the gel rotated by 90°, as described by Cilley and Williamson (32). The total concentration of 5′-^{32}P labeled RNA was 10 μM.

RESULTS

Identification of the binding sites by NMR

The C1′/H1′, C5/H5, C6/H6 and C8/H8 RNA resonances were monitored upon titration of the ligand in concentration ratios varying from 1:1 to 1:100. Significant chemical shift changes were observed up to a 10-fold excess of the ligand (3 mM) over the RNA (0.3 mM), indicating that the equilibrium dissociation constant K_d is in the micromolar range or higher. The chemical shift mapping identifies A22, U23 and the loop nucleotides G32, G34 and A35 as the sites being most affected by the binding of the aminoglycoside analog **1** (Figure 1). In agreement with this observation, binding of ligand **1** protects both loop sites G32–G34 and C30 from digestion with RNase T1 and with RNAse A, respectively (Figure 2). These data suggest a large and unprecedented change in the loop conformation upon binding of a positively charged molecule to the TAR-RNA, which motivated the choice of studying the TAR/**1** complex.

The intermolecular NOESY spectrum reveals intimate contacts of ligand **1** with A22, U23, U25 and A35. The atypical C8/H8 chemical shifts of A35 in the free TAR-RNA implies that the adenosine base is partially projected out of the loop, thus occupying an optimal position for interacting with a ligand bound to the bulge on the side of the upper stem major groove. Large chemical shifts changes are observed upon titration of ligand **1** for the C2/H2 and C1′/H1′ resonances of A35. In particular, the linewidth of the A35–C2 decreases
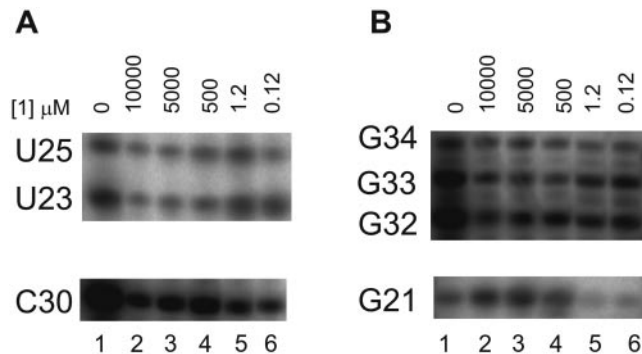

Figure 2. RNase footprinting. RNase protection assays of the TAR/**1** complex were carried out with 10 μM 5′-^{32}P-labeled HIV-2 TAR-RNA at 4°C. The digestion experiments were analyzed by gel electrophoresis. (**A**) Digestion with RNase A (selective for C and U). Lane 1, control without RNase; lane 2, compound **1** (10 mM); lane 3, compound **1** (5 mM); lane 4, compound **1** (500 μM); lane 5, compound **1** (1.2 μM); lane 6, compound **1** (0.12 μM). (**B**) Digestion with RNase T1 (G selective). Lane 1, control without RNase; lane 2, compound **1** (10 mM); lane 3, compound **1** (5 mM); lane 4, compound **1** (500 μM); lane 5, compound **1** (1.2 μM); lane 6, compound **1** (0.12 μM).

from 80 to 48 Hz at 900 MHz, which suggests that in free TAR this nucleotide assumes different conformations interchanging on a μs to ms time scale, while in the complex the base occupies a well-defined position. Notable is the chemical shift change experienced by the base of G34, which varies the most upon formation of the complex without showing any direct contact to the ligand. This is indicative of a profound change in the electronic environment of G34 and, possibly, of the overall conformation of the loop, triggered by the interaction of A35 with **1**. The chemical shift change of G34-C8/H8 is accompanied by a considerable decrease in the transverse relaxation time T_2 of G34-C8, indicating that G34, which is disordered in the free TAR and in the TAR/argininamide complex (33,34), undergoes a slow (μs–ms time scale) conformational transition between two states in complex with **1**. Considerable chemical shifts changes are observed also for the riboses of U31, G32 and G33. Clearly, binding of the aminoglycoside analog to A35 triggers a profound conformational change in the hexanucleotide loop, which moves from a completely disordered state to a partially ordered one.

In the bulge, the largest chemical shift changes are observed for A22 and U23. U23 stacks on A22 in the free TAR-RNA (33), while in this complex it is involved in several contacts with the aminoglycoside analogue **1**. The A22–U40 base pair, which is stably formed at low temperature in the HIV-2 TAR-RNA, is disrupted in the complex, as confirmed by the failure to observe the U40 imino resonance even at 4°C. However, several NOEs indicate that both A22 and U40 remain positioned between G21/G26 and C39/C41, respectively.

A35 is the only loop residue that directly contacts the ligand, suggesting that the interaction of **1** with the loop must be part of a more complex network of interactions holding the complex together. Cooperative binding of **1** to both the loop and the bulge of the TAR-RNA is supported by the chemical shift data, which indicate a K_d of comparable size for both the bulge and the loop sites. Moreover, while **1**

inhibits the binding of Tat-derived peptides to the TAR-RNA, linear analogues or smaller cyclic analogues of **1** do not show any biological activity (35), underlining the importance of a cyclic constrained structure of appropriate size for the cooperative binding to the bulge and loop regions of the RNA. Therefore, it is safe to conclude that one molecule of ligand **1** binds simultaneously to the loop and the bulge of the RNA.

A medium-sized chemical shift change of G43–C1′ upon titration of **1**, together with NOEs between the aminoglycoside analogue **1** and both G43-H1′ and G44-H4′, reveal an additional binding site of **1** in the minor groove of the RNA lower stem. This finding is not surprising, as structural studies of the TAR/neomycin B complex (15) had identified the lower stem minor groove as a binding site for positively charged aminoglycosides.

Compound **1** can be produced with ^{15}N and ^{13}C labeling at reasonable cost. In the course of this study we produced a ^{15}N-labeled batch of compound **1** (25) with the aim of verifying the existence of H-bonds between the amino groups of the aminoglycoside analogue and the RNA phosphates by detection of H-bond mediated ^{15}N-^{31}P scalar couplings. Unfortunately, no such coupling could be observed for the degenerate amino group.

Structure calculations including NOEs and dihedral angle restraints were first conducted on a monomeric unit containing one TAR molecule and one ligand molecule binding to the upper stem (Supplementary Data). The final ensemble of 50 structures defines the binding site in the upper stem major groove, where the most profound contacts between the RNA and ligand **1** are situated.

Analysis of the dipolar couplings and dimerization

A few dipolar couplings of the base C–H atom pairs measured at 800 MHz assume values between −5 and −6 Hz. These figures exceed by far those expected for the TAR-RNA aligned in the magnetic field due to the magnetic susceptibility anisotropy of the bases (36). The largest dipolar coupling tensor is expected for coaxial stacking of the upper and lower stems and would correspond to a D_{zz} of 8 Hz and a rhombicity R between 0 and 0.1 in an 800 MHz field. For such tensor, the largest base C–H dipolar coupling should not exceed −4 Hz. The high values found for the TAR/**1** complex suggest that the RNA dimerizes in the presence of the ligand (37). The experimental dipolar couplings of the two stems can be best fitted to the ensemble of 50 structures, derived from NOE and dihedral angle restraints, by assuming a D_{zz} of 7 Hz and an R of 0.55. The interstem angle after refinement with the RDCs is ~60°. The experimentally determined dipolar coupling tensor fits well that predicted for a dimeric TAR-RNA where the upper and lower stems of each unit form an angle of 60° and the two RNA molecules are associated with two of their stems approximately parallel to each other and the other two stems pointing in opposite directions (36).

The 3D ^{13}C-edited/^{12}C-filtered HSQC-NOESY spectrum in D$_2$O and the 3D ^{13}C-edited/^{12}C/^{14}N-filtered HSQC-NOESY in H$_2$O recorded on a sample containing 150 μM ^{13}C/^{15}N labelled RNA, 150 μM unlabeled RNA and 3 mM ligand showed no intermolecular NOEs between two TAR-RNA molecules. This finding indicates that no direct contact between the two RNA molecules takes place in the dimer and hence the dimerization must be mediated by one or more aminoglycoside molecules. The presence of only one set of resonances for the RNA further indicates that the complex is symmetric.

The dipolar couplings define the relative orientation of the two RNA units. However, it remains to be defined if the two RNA molecules associate through the aminoglycoside molecule bound to the upper stem major groove site or to the lower stem minor groove site. Structure calculations with NOE and dihedral restraints were conducted for both cases: association through the molecule of **1** bound to the upper stem site resulted in large NOE violations and high energy due to severe distortion of the aminoglycoside. Therefore, only dimerization through one molecule of **1** bound to the lower stem minor groove is compatible with the NOE data. With these constraints, a molecule of the aminoglycoside analogue **1** was docked into the minor groove of the lower stem of two TAR-RNA molecules, which were predisposed in the correct orientation to reproduce the experimentally derived dipolar coupling tensor.

PACE gel electrophoresis (32) was used to verify the stoichiometry of the complex. As shown in Figure 3, the PACE data could be poorly fitted assuming monomeric RNA (i, ii, iv) or formation of a dimer with one or two molecules of **1** (iii, v). Instead, a good fit of the retardation distances was obtained assuming a dimerization step including two RNA molecules and one molecule of **1**, followed by subsequent recruitment of two additional molecules of the aminoglycoside (red curve, case vi), which supports the dimer geometry inferred from the NMR data.

Interestingly, the longitudinal relaxation rates R_1 of the base carbons of the TAR-RNA decreased in complex with **1** by ~40%. This decrease cannot be explained by invoking internal dynamics, as it affects also the carbons of the stem bases, whose structure remains unchanged upon binding of **1**. Instead, the smaller relaxation rates may indicate a change in the overall correlation time of the TAR-RNA, which also supports the dimerization model.

The upper stem-binding site

The structure calculation employing NOEs and dihedral angle restraints, conducted on a monomeric unit containing one TAR and one ligand molecule binding to the upper stem, resulted in a well-defined structure in both stems but in a poor definition of the relative orientation of the two stems [root mean square deviation (r.m.s.d.) for the lower stem, 0.5 Å; r.m.s.d. for the upper stem, 0.8 Å]. The structure refinement with the C–H *fi*RDCs positioned the two stems at a relative angle of ~60°.

The 14 lowest-energy structures of the monomeric unit are shown in Figure 4. The RNA is well defined with a total heavy atom r.m.s.d. (excluding the loop residues) of 0.92 Å. The A-form helix structure of the lower (nt 16–21, 41–46) and upper (nt 26–29, 36–39) stems is conserved. The upper stem helix is, however, slightly distorted, with the α and γ angles varying from the typical A-form *gauche −* and *gauche +* conformations to the *trans* conformation for residues A27–C29 and C39.
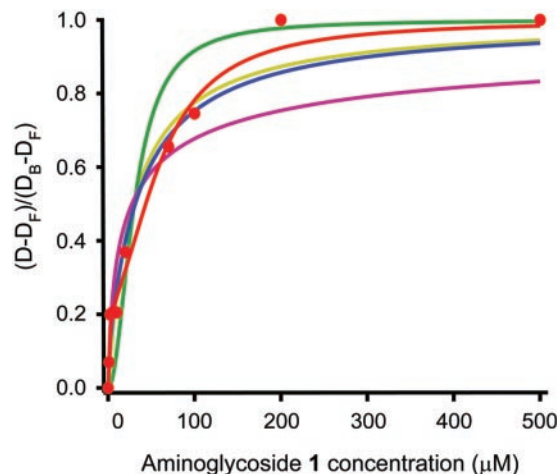
Figure 3. Binding stoichiometry. The function $(D - D_F)/(D_B - D_F)$ is plotted versus the concentration of the aminoglycoside analogue **1** in each lane of the PACE gel. D is the retardation distance in each lane, D_F is the retardation distance of the TAR-RNA without **1** and D_B is the retardation distance of the TAR-RNA completely bound to **1** (concentration of **1** = 500 μM). The function $(D - D_F)/(D_B - D_F)$ can be expressed in terms of molar fractions of bound and free RNA, according to the procedure described by Cilley and Williamson (32). Different binding models were assumed and the theoretical dependence of $(D - D_F)/(D_B - D_F)$ on the concentration of **1** was calculated in each case from the molar fractions assuming constant concentration of **1** in each lane. The experimental data (red dots) were fitted to the theoretical functions using IgorPro to derive the binding stoichiometry for the TAR/**1** complex. Six different models were considered: (i) one molecule of the TAR-RNA binds one molecule of **1** (yellow line); (ii) one molecule of the TAR-RNA binds two molecules of **1** with the same K_d (green line); (iii) two molecules of the RNA bind one molecule of **1** (magenta); (iv) one molecule of the TAR-RNA binds two molecules of **1** with different K_d (blue line); (v) one molecule of the TAR-RNA binds one molecule of **1** ($TAR + 1 \xleftrightarrow{k_{d1}} C_1$); subsequently the TAR/**1** complex dimerizes ($2C_1 \xleftrightarrow{k_{d2}} C_2$) (close to the yellow line, not shown); (vi) two molecules of the RNA bind one molecule of **1** ($2\ TAR + 1 \xleftrightarrow{k_{d1}} C_1$); subsequently two molecules of **1** are recruited by the RNA dimer for a total of two RNA molecules and three molecules of **1** ($C_1 + 2\,1 \xleftrightarrow{k_{d2}} C_2$) (red line; $K_{d1} \approx 20$ μM^2; $K_{d2} \approx 3$ mM^2). The best fit is obtained for case (f), which supports the stoichiometry inferred from the NMR data.

The aminoglycoside analogue **1** binds to the bulge and the loop residues on the major groove side of the upper stem (Figures 4 and 5). Owing to the 4-fold symmetry of its resonances and the fast kinetics of complex dissociation, the structure of **1** in the complex cannot be determined. However, the salient features of the interaction between the aminoglycoside analogue **1** and the TAR-RNA are well defined and the r.m.s.d. of the whole complex excluding the loop residues 30–34 is 1.2 Å.

The backbone of the 22–25 stretch opens up to allow **1** to reach the major groove of the RNA upper stem (Figure 4). The last base pair of the lower stem is disrupted: U40 stacks below C39; A22 stacks below G26 but tilts away from U40 to widen the major groove of the upper stem and make place for the ligand. Thus, in the TAR/**1** complex, A22 and U40 belong to the upper stem, while in free TAR they stack on the top of the lower stem G21–C41 base pair. In agreement with the disruption of the A-form helix structure between G21 and A22, the digestion of the TAR-RNA at the G21 site by RNase T1 increases upon titration of **1** (Figure 2B). The planarity of the G26–C39 base pair
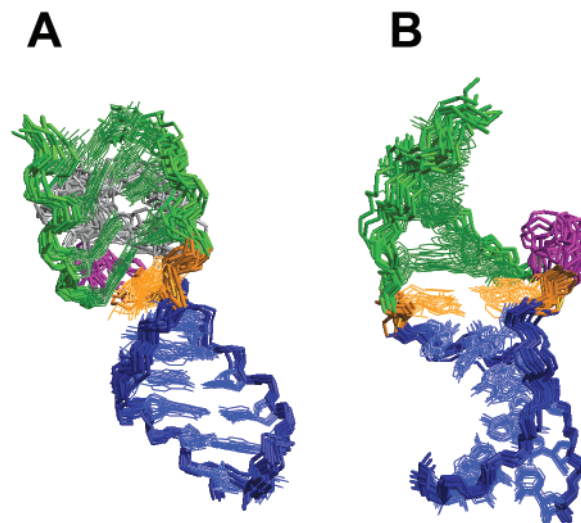

Figure 4. Structure of the TAR/**1** complex. (**A**) Superposition of the heavy atoms of 14 structures of the TAR/**1** complex based upon residues 16–21, 26–29 and 36–46. These structures had total energy <−300 kcal/mol, no NOE violations >0.5 Å and no angular violations. Residues 30–35 and the bases of U23/U25 are not shown. The lower stem is colored in blue and the upper stem in green. A22 and U40 are highlighted in orange; the backbone of the bulge is in magenta. The backbone and the base stacking indicate that the upper and lower stems form an angle of ∼60°. The aminoglycoside binding to the major groove of the HIV-2 TAR-RNA upper stem is rendered in gray. (**B**) Same ensemble as in (A) after 180° rotation around the vertical axis. The ligand is not shown.

is slightly distorted, as indicated by the weakening of the G26 imino resonance upon complex formation. The π-orbitals of the U23 and U25 bases entertain hydrophobic interaction with linker-*4* and sugar-*3*/linker-*2* of ligand **1**, respectively (Figure 5). Such hydrophobic contacts resemble a well-known interaction motif in complexes of proteins with oligosaccharides, where the sugars often stack below aromatic side chains (38).

The conformation induced by ligand **1** at the bulge site of the TAR-RNA, as well as the relative orientation of the two stems, differ from those found in the Tat/TAR complex. Binding of **1** does not induce either the formation of the U23–A27–U38 base triple or the subsequent coaxial stacking of the upper and lower stems, as it is the case for the binding of the Tat mimetic argininamide (34). Instead, the bulge nucleotides are all exposed to the solvent in the TAR/**1** complex and the axes of the two stems form an angle of ∼60°. The relative position of the two domains is probably a consequence of the disruption of the A22–U40 base pair, of the tilting of A22 to accommodate the large ligand and of the electrostatic interactions of the ligand amino group with the phosphate of A22.

A35 stacks on the top of the sugar-*1* moiety of the ligand and is involved in a π-cation interaction with the positively charged amino group. This contact pulls A35 out of the loop, causing G34 to move on the top of G36 in all structures. In 60% of the structures G34 stacks on the top of G36, while in the other 40% the two bases interact face-to-edge (Figure 6). The presence of an equilibrium between two conformations is compatible with the large linewidth of the G34–C8 resonance, suggesting that the exchange between
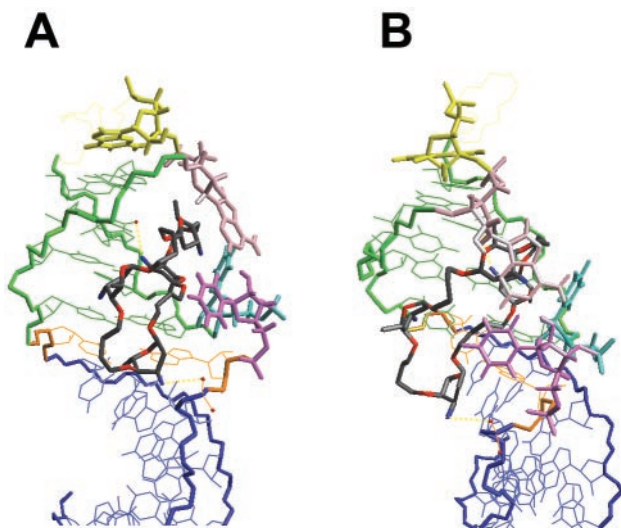
Figure 5. The aminoglycoside analogue **1** binds to the upper stem major groove. (**A**) View of the best energy structure of the family of Figure 4. The aminoglycoside analogue **1** (color coded by atom: dark gray, red and blue sticks) is placed in the major groove of the upper stem of the HIV-2 TAR-RNA. A22 and U40, depicted in orange, clearly show that the hydrogen bonds between 22 and 40 are disrupted and that A22 tilts away from the major groove to accommodate the ligand. Besides A22 and G26, U23 (magenta), U25 (turquoise) and A35 (pink) have direct contacts with the aminoglycoside analogue. The positively charged amino group of the ligand sugar-*1* interacts with the π-orbital of the A35 base, the amino group of sugar-*3* interacts electrostatically with the major groove edge of G28 (dashed yellow line), while the amino group of sugar-*5* contacts the phosphate of A22 (dashed yellow line). G34 (yellow sticks) stacks on the top of G36. The backbone of the loop is shown as yellow lines. A similar intermolecular interaction pattern is observed also for the other structures of the ensemble. (**B**) Same as in (A) after 90° rotation around the vertical axis.
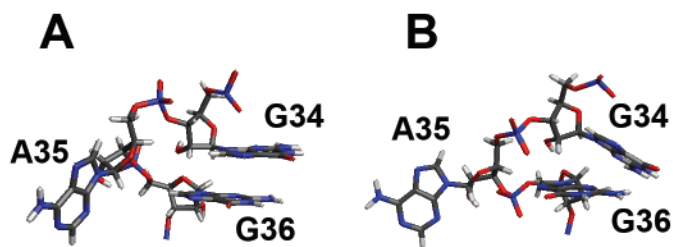

Figure 6. G34 is positioned on the top of G36. A35 interacts with the ligand and therefore moves out of the loop. As a consequence, G34 moves on the top of G36. The two bases interact either face-to-face (**A**) or face-to-edge (**B**). The two conformations are likely to be in intermediate exchange (μs–ms time scale), as inferred from the linewidth of the G34–C8 resonance.

the face-to-face and face-to-edge orientations of G34 and G36 occurs on a μs–ms time scale.

The positively charged amino groups of the four sugars of ligand **1** interact with various functional groups of the RNA (Figure 5). The amino group of sugar-*1* (Scheme 1) is involved, as already mentioned, in a π-cation interaction with A35 and in long-range electrostatic interactions with the O2 of U25. The amino group of sugar-*3* is directed towards the major groove carbonyls of the A27–U38 and G28–C39 base pairs in all structures but two, while the amino group of sugar-*5* is close to the phosphate backbone
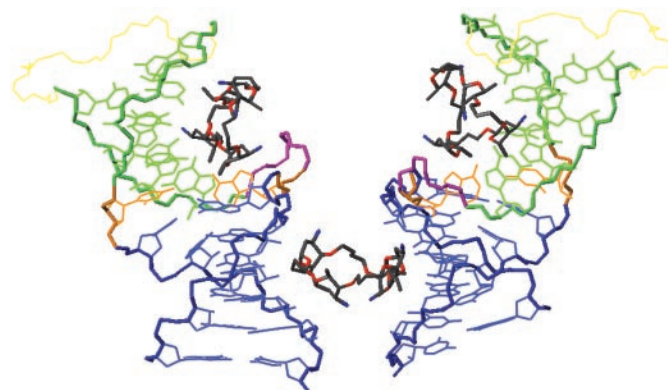

Figure 7. Model for the dimerization of the TAR/1 complex. The TAR-RNA with one molecule of **1** bound to the upper stem major groove dimerizes through an aminoglycoside molecule bound to the lower stem minor groove. The two RNA molecules are oriented with the lower stems roughly parallel to each other (interhelical angle $\theta \approx 30°$) and the upper stems diverging from each other. From the magnetic susceptibility tensor of the dimeric RNA a dipolar coupling tensor can be calculated (D_{zz}, 6.8 Hz; R, 0.54), which fits well the experimentally determined one (36). The color-coding is the same as in Figure 5.

of A22 and/or to the O4 of U23. Finally, no consistent contact is found for the amino group of sugar-*7*. These results are in agreement with the failure to detect H-bonding of the amino groups of ligand **1** to the phosphate backbone of the RNA by the J_{NP} scalar coupling measurement, as most of the amino groups of the ligand contact base functional groups rather than phosphates.

Definition of the second binding site and of the dimer geometry

Similar to neomycin (15), the aminoglycoside analogue **1** binds also to the minor groove of the lower stem of the TAR-RNA. The chemical shift change of G43–C1′ is maximum at a 1:1 ratio of RNA:aminoglycoside, as opposed to the chemical shift changes in the bulge and loop region, which increase up to a 1:10 ratio. Thus, the binding constant of **1** to the minor groove of the TAR-RNA is higher than that to the bulge and loop regions. This finding is confirmed by the analysis of the PACE data (see caption of Figure 3).

The *fi*RDC data suggested association of two TAR/**1** units with two stems of the two RNA molecules in a roughly parallel orientation and the other two stems diverging from each other. We identified dimer formation through the aminoglycoside bound to the lower stem minor groove as the only one consistent with the NOE data. The model shown in Figure 7 is compatible with all experimental data, including NOEs, relaxation rates, *fi*RDCs and PACE gel electrophoresis. In this model, the aminoglycoside analogue **1** binds almost symmetrically to the minor groove of the lower stems of the two TAR-RNA units. One amino group enjoys electrostatic interactions with the negative spot created by the phosphate groups of G21, A22 and U23, while another amino group closely contacts the 2′-hydroxyl of C45. Two sugars and the intervening linker of **1** penetrate the minor groove of each RNA molecule at the G43–C45 site (Figure 7).

DISCUSSION

Binding of 1 to multiple spots of the upper stem major groove

It is widely recognized that the intermolecular surface in RNA/protein complexes is rather large and therefore small molecules cannot efficiently compete with proteins for RNA binding. Despite many efforts in the search for competitive inhibitors of the Tat/TAR interaction, no drug lead has been identified to date. The major difficulty in the development of TAR-binders as potential therapeutic agents is their low specificity. The problem might be alleviated by simultaneously targeting multiple binding sites on the TAR-RNA (39,40). An extended effort in identifying the minimal number of interactions necessary to stabilize the Tat-bound conformation of the TAR-RNA resulted in the detection of two binding sites for positively charged groups at the bulge site and in the upper stem major groove close to A27 and G28 (40). Synthetic ligands exploiting both binding sites showed the highest activity and induced an RNA conformation similar to that binding to the Tat-protein (40). The amino groups of ligand **1** contact both the bulge site and the major groove functional groups at the G28 site (Figure 5). Although the interaction with the bulge is suboptimal and could be improved by introducing a guanidinium group at the C1 or C5 of sugar-*5*, the amino group of sugar-*3* nicely interacts with the electron-rich spot at the G28 and U38 site (Figure 5). Additionally, the amino group of sugar-*1* interacts with the loop residue 35. Thus, the large but flexible scaffold of **1** allows reaching multiple binding sites on the TAR-RNA, and therefore represents a valuable starting structure for the design of binders that explore a large surface of the TAR upper stem.

Cyclic scaffold of 1

The value of cyclic structures as a conformationally constrained backbone for TAR binders has been proven by the design of peptidomimetics based on a cyclic, β-hairpin-like scaffold (29), binding the TAR-RNA with a much higher affinity than the linear analogs (41). The structure of the BIV (bovine immunodeficiency virus) TAR-RNA bound to one of these peptidomimetics revealed extensive interactions with the upper stem major groove, including a conserved hydrophobic contact of an Ile residue with the bulged-out U of the base triple as well as electrostatic contacts of arginine side chains with the tetraloop capping the upper stem and with the second and third base pairs of the upper stem (29). Intermolecular interactions of similar nature are found for the TAR/**1** complex. Analogously to the BIV TAR-RNA/peptide complex, ligand **1** uses hydrophobic contacts to bind to the bulge pyrimidines and electrostatic contacts to bind to the major groove face of the upper stem base pairs and to the loop residues. As observed for the peptides, linear neooligoaminodeoxysaccharides show a much lower affinity for the TAR-RNA than their cyclic analog **1** (25).

The binding of 1 induces a conformational change in the loop of the TAR-RNA

The hexanucleotide apical loop has been found to be quite flexible in all NMR studies (42–44), with the riboses of C30, G33 and G34 averaging between the C2′-*endo* and the C3′-*endo* conformations. Base stacking of A35 on G36 and of G34 on G36 was found to be consistent with structural restraints derived by NMR for a 14 and a 19 nt hairpin containing the TAR hexanucleotide loop (43,44). On the basis of such structural information, it was proposed that the apical loop is stabilized by base stacking on both sides and possibly by the formation of base pairs between C30 and A35$^+$ or C30 and G34 (43). In a more recent work, biochemical analysis of native and mutant TAR-RNAs was used together with MD simulations to show that the apical loop of the TAR-RNA is stabilized by a cross-loop base pair between C30 and G34, with A35 projected out of the loop (45). This observation does not necessarily contradict the NMR studies hypothesizing the stacking of A35 on G36. The large line-broadening of the A35–C2 resonance of the free TAR-RNA and the NOEs between the bases of G34, A35 and G36 are consistent with A35 being in equilibrium between the stacked and looped-out conformations.

This equilibrium is not present in the complex. Upon binding of **1** the NOE contacts between the base of A35 and both G34 and G36 disappear, while several NOEs appear between G34 and G36, indicating stacking of G34 on G36. In the stacked conformation, the formation of the C30–G34 base pair becomes possible; however, no evidence of this base pair could be found in the TAR/**1** complex. The ribose pucker of G34 assumes the C3′-*endo* conformation in the complex, in agreement with MD simulations, where the C3′-*endo* pucker of the G34 ribose has been found to accompany the stacking of G34 upon G36 (45). All in all, our data indicate that binding of a positively charged ligand of appropriate size to the bulge and the loop of the TAR-RNA on the major groove side of the upper stem leads to the stabilization of the looped-out conformation of A35 and, consequently, to the relocation of G34 on G36.

Comparison of the TAR/1 complex with the binding of CycT1 to the TAR loop

The formation of the Tat/TAR complex is required for the recruitment of the P-TEFb complex and for the phosphorylation and subsequent activation of the RNA polymerase stalled at the TAR-RNA site. The P-TEFb complex consists of the kinase component CDK9 and the cyclin T1 subunit (CycT1) and binds to the TAR-RNA through the CycT1 subunit in a Tat-dependent manner. The interaction site of CycT1 with the TAR-RNA is localized in the apical loop. The two atoms O6 and N7 of G34 and G32 and the presence, but not the nature, of a nucleotide in position 35 are essential for the interaction (4). The mechanism by which the Tat protein favors the interaction of CycT1 with the apical loop is not known, although it is reasonable to hypothesize that Tat structurally pre-organizes the RNA for the binding of CycT1.

On the basis of the structure of the complex of TAR with the aminoglycoside analogue **1**, we propose an explanation for the dependence of the TAR/CycT1 interaction on the Tat/TAR complex formation, which fits well the biochemical data summarized above. We suggest that the binding of Tat to TAR pre-organizes the hexanucleotide loop in a favorable conformation for CycT1 binding. It is conceivable that the

arginine-rich stretch of the Tat protein, which is responsible for TAR binding at the bulge site, also contacts the A35 residue of the hexanucleotide loop and blocks it in its looped-out conformation, in a similar way as our aminoglycoside. The major driving force for this contact could be the interaction of an aromatic π orbital with a cation, similarly to that observed for the TAR/**1** complex. A generic π-cation interaction provides a rationale for the insensitivity of the TAR/CycT1 interaction to the nature of the nucleotide in position 35. A small negative effect on complex formation is observed exclusively for the A35G mutant, where a possible cross-loop C30–G35 base pair would destabilize the looped-out conformation of the nucleotide in position 35. Supporting our hypothesis, affinity cleaving experiments show that F38 of Tat is located in the proximity of nt 34 and 35 of the TAR-RNA (46). Furthermore, the residue K50 of the Tat-protein has been found to cross-link with the TAR nt 34, and this interaction is considerably enhanced by the binding of CycT1 to the Tat/TAR complex (4).

In the TAR/**1** complex, the looped-out conformation of A35 is accompanied by the relocation of G34 upon G36. Analogously, in the Tat/TAR complex stacking of G34 upon G36 would place the O6 and N7 atoms of G34, which are essential for the binding of CycT1, in a well-defined position in the major groove of the TAR-RNA. The formation of a base pair between C30 and G34 would further stabilize the position of the G34 functional groups. In fact, such base pair has been shown to favor the interaction of the TAR-RNA with CycT1 without being directly involved in the complex formation (4).

Based on the irrelevance of the nucleotide nature at position 35, it has been hypothesized that this nucleotide functions as a spacer with no direct contact to the proteins. Contrarily, we suggest that A35 could be the basis of a regulation mechanism for the formation of the Tat/TAR/CycT1 complex based on the conformational stability of the hexanucleotide loop.

The lower stem-binding site and dimerization

The aminoglycoside analogue **1** binds also to the minor groove of the lower stem of the TAR-RNA, similar to neomycin B (15). Furthermore the TAR/**1** complex dimerizes. A model invoking oligomerization of the TAR/**1** complex through the molecule of **1** bound to the lower stem minor groove is compatible with all experimental data. This process is likely to be entropy-driven and favored by the constrained cyclic structure of **1**.

Significance for drug design

The design of drug leads targeting the TAR-RNA has focused almost exclusively on the inhibition of the Tat/TAR interaction at the bulge site. However, the TAR/**1** complex structure suggests that a cyclic scaffold can be used to design ligands that extensively bind to the entire upper stem major groove of the TAR-RNA up to the capping loop. The interaction with A35 might be a general feature of large ligands binding to the major groove of the TAR-RNA, as supported by an NOE identified in a previous study between a compound binding to TAR in a Tat-similar manner and the A35–H8 (40). The cyclic scaffold of ligand **1** can be utilized in the design of TAR binders, which capture A35 in the looped-out conformation, induce the relocation of G34 on the top of G36 and are decorated with appropriate functional groups to compete with CycT1 for the G34 functional groups. Large ligands, interfering with both the Tat/TAR and the Tat/TAR/CycT1 complex formation, could represent an improved class of drug leads both in terms of efficiency and specificity.

CONCLUSIONS

We have presented the 3D structure of the TAR-RNA in complex with a novel macrocyclic aminoglycoside analogue. One of the two ligand binding sites spans from the bulge to the loop of the TAR-RNA on the side of the upper stem major groove, thus obstructing a large part of it. In particular, the aminoglycoside analogue **1** interacts with the residue A35 of the RNA capping loop, thereby inducing partial structuring of the loop. We suggest that this conformational change observed in the loop of TAR upon binding of **1** resembles the restructuring of the loop required for CycT1 binding and that this restructuring is induced by Tat. On the basis of the structural information obtained in this study, we believe that the aminoglycoside analogue **1** holds promises to be used as a scaffold for the design of a new generation of TAR binders that can inhibit both the Tat/TAR and Tat/TAR/CycT1 complex formation.

ACKNOWLEDGEMENTS

REFERENCES

1. Frankel,A.D. (1992) Activation of HIV transcription by Tat. *Curr. Opin. Genet. Dev.*, **2**, 293–298.
2. Wei,P., Garber,M.E., Fang,S.M., Fischer,W.H. and Jones,K.A. (1998) A novel CDK9-associated C-type cyclin interacts directly with HIV-1 Tat and mediates its high-affinity, loop-specific binding to TAR RNA. *Cell*, **92**, 451–462.
3. Garber,M.E., Wei,P., KewalRamani,V.N., Mayall,T.P., Herrmann,C.H., Rice,A.P., Littman,D.R. and Jones,K.A. (1998) The interaction between HIV-1 Tat and human cyclin T1 requires zinc and a critical cysteine residue that is not conserved in the murine CycT1 protein. *Genes Dev.*, **12**, 3512–3527.
4. Richter,S., Cao,H. and Rana,T.M. (2002) Specific HIV-1 TAR RNA loop sequence and functional groups are required for human cyclin Tl-Tat-TAR ternary complex formation. *Biochemistry*, **41**, 6391–6397.
5. Roy,S., Delling,U., Chen,C.H., Rosen,C.A. and Sonenberg,N. (1990) A bulge structure in HIV-1 TAR RNA is required for Tat binding and Tat-mediated transactivation. *Genes Dev.*, **4**, 1365–1373.
6. Cordingley,M.G., Lafemina,R.L., Callahan,P.L., Condra,J.H., Sardana,V.V., Graham,D.J., Nguyen,T.M., Legrow,K., Gotlib,L., Schlabach,A.J. *et al.* (1990) Sequence-specific interaction of Tat protein and Tat peptides with the transactivation-responsive sequence element of human-immunodeficiency-virus type-1 *in vitro*. *Proc. Natl Acad. Sci. USA*, **87**, 8985–8989.

7. Weeks,K.M. and Crothers,D.M. (1991) RNA recognition by Tat-derived peptides—interaction in the major groove. *Cell*, **66**, 577–588.

8. Arzumanov,A., Walsh,A.P., Liu,X.H., Rajwanshi,V.K., Wengel,J. and Gait,M.J. (2001) Oligonucleotide analog interference with the HIV-1 Tat protein–TAR RNA interaction. *Nucleosides Nucleotides Nucleic Acids*, **20**, 471–480.

9. Kaushik,N., Basu,A., Palumbo,P., Myers,R.L. and Pandey,V.N. (2002) Anti-TAR polyamide nucleotide analog conjugated with a membrane-permeating peptide inhibits human immunodeficiency virus type 1 production. *J. Virol.*, **76**, 3881–3891.

10. Mischiati,C., Jeang,K.T., Feriotto,G., Breda,L., Borgatti,M., Bianchi,N. and Gambari,R. (2001) Aromatic polyamidines inhibiting the Tat-induced HIV-1 transcription recognize structured TAR-RNA. *Antisense Nucleic Acid Drug Dev.*, **11**, 209–217.

11. Hermann,T. and Westhof,E. (1998) Saccharide-RNA recognition. *Biopolymers*, **48**, 155–165.

12. Mei,H.Y., Cui,M., Heldsinger,A., Lemrow,S.M., Loo,J.A., Sannes-Lowery,K.A., Sharmeen,L. and Czarnik,A.W. (1998) Inhibitors of protein–RNA complexation that target the RNA: Specific recognition of human immunodeficiency virus type 1 TAR RNA by small organic molecules. *Biochemistry*, **37**, 14204–14212.

13. Mei,H.Y., Galan,A.A., Halim,N.S., Mack,D.P., Moreland,D.W., Sanders,K.B., Truong,H.N. and Czarnik,A.W. (1995) Inhibition of an HIV-1 Tat-derived peptide binding to TAR RNA by aminoglycoside antibiotics. *Bioorg. Med. Chem. Lett.*, **5**, 2755–2760.

14. Wang,S.H., Huber,P.W., Cui,M., Czarnik,A.W. and Mei,H.Y. (1998) Binding of neomycin to the TAR element of HIV-1 RNA induces dissociation of Tat protein by an allosteric mechanism. *Biochemistry*, **37**, 5549–5557.

15. Faber,C., Sticht,H., Schweimer,K. and Rosch,P. (2000) Structural rearrangements of HIV-1 Tat-responsive RNA upon binding of neomycin B. *J. Biol. Chem.*, **275**, 20660–20666.

16. Wilson,W.D. and Li,K. (2000) Targeting RNA with small molecules. *Curr. Med. Chem.*, **7**, 73–98.

17. Michael,K. and Tor,Y. (1998) Designing novel RNA binders. *Chem. Eur. J.*, **4**, 2091–2098.

18. Mingeot-Leclercq,M.P. and Tulkens,P.M. (1999) Aminoglycosides: nephrotoxicity. *Antimicrob. Agents Chemother.*, **43**, 1003–1012.

19. Chen,G.W. and Kirschning,A. (2002) First preparation of spacer-linked cyclic neooligoaminodeoxysaccharides. *Chem. Eur. J.*, **8**, 2717–2729.

20. Bax,A., Ikura,M., Kay,L.E., Torchia,D.A. and Tschudin,R. (1990) Comparison of different modes of 2-dimensional reverse-correlation NMR for the study of proteins. *J. Magn. Res.*, **86**, 304–318.

21. Wijmenga,S.S. and van Buuren,B.N.M. (1998) The use of NMR methods for conformational studies of nucleic acids. *Prog. Nucl. Magn. Reson. Spectrosc.*, **32**, 287–387.

22. Leupin,W., Otting,G., Amacker,H. and Wuthrich,K. (1990) Application of C-13(Omega-1)-Half-Filtered [H-1,H-1]-NOESY for studies of a complex formed between DNA and a C-13-labeled minor-groove-binding drug. *FEBS Lett.*, **263**, 313–316.

23. Brutscher,B., Boisbouvier,J., Kupce,E., Tisne,C., Dardel,F., Marion,D. and Simorre,J.P. (2001) Base-type-selective high-resolution C-13 edited NOESY for sequential assignment of large RNAs. *J. Biomol. NMR*, **19**, 141–151.

24. Schwalbe,H., Marino,J.P., King,G.C., Wechselberger,R., Bermel,W. and Griesinger,C. (1994) Determination of a complete set of coupling-constants in C-13-labeled oligonucleotides. *J. Biomol. NMR*, **4**, 631–644.

25. Jaunzems,J., Oelze,B. and Kirschning,A. (2004) Preparation of macrocyclic N-15-labelled oligoaminodeoxysaccharides as probes for RNA-binding. *Org. Biomol. Chem.*, **2**, 3448–3456.

26. Vuister,G.W. and Bax,A. (1993) Quantitative J correlation—a new approach for measuring homonuclear 3-bond J(H(N)H(Alpha) coupling-constants in N-15-enriched proteins. *J. Am. Chem. Soc.*, **115**, 7772–7777.

27. Bastiaan,E.W. and MacLean,C. (1991) Molecular orientation in high-field high-resolution NMR. *Basic. Princ. Prog.*, **25**, 17–43.

28. Schwieters,C.D., Kuszewski,J.J., Tjandra,N. and Clore,G.M. (2003) The XPLOR-NIH NMR molecular structure determination package. *J. Magn. Res.*, **160**, 66–74.

29. Leeper,T.C., Athanassiou,Z., Dias,R.L.A., Robinson,J.A. and Varani,G. (2005) TAR RNA recognition by a cyclic peptidomimetic of Tat protein. *Biochemistry*, **44**, 12362–12372.

30. Meiler,J., Peti,W. and Griesinger,C. (2000) DipoCoup: a versatile program for 3D-structure homology comparison based on residual dipolar couplings and pseudocontact shifts. *J. Biomol. NMR*, **17**, 283–294.

31. Koradi,R., Billeter,M. and Wuthrich,K. (1996) MOLMOL: a program for display and analysis of macromolecular structures. *J. Mol. Graph.*, **14**, 51–55, 29–32.

32. Cilley,C.D. and Williamson,J.R. (1997) Analysis of bacteriophage N protein and peptide binding to boxB RNA using polyacrylamide gel coelectrophoresis (PACE). *RNA*, **3**, 57–67.

33. Aboulela,G., Karn,J. and Varani,G. (1996) Structure of HIV-1 TAR RNA in the absence of ligands reveals a novel conformation of the trinucleotide bulge. *Nucleic Acids Res.*, **24**, 4598–4598.

34. Brodsky,A.S. and Williamson,J.R. (1997) Solution structure of the HIV-2 TAR-argininamide complex. *J. Mol. Biol.*, **267**, 624–639.

35. Kirschning,A., Chen,G.W., Jaunzems,J., Jesberger,M., Kalesse,M. and Lindner,M. (2004) Synthesis of extended spacer-linked neooligodeoxysaccharides by metathesis olefination and evaluation of their RNA-binding properties. *Tetrahedron*, **60**, 3505–3521.

36. Zhang,Q., Throolin,R., Pitt,S.W., Serganov,A. and Al-Hashimi,H.M. (2003) Probing motions between equivalent RNA domains using magnetic field induced residual dipolar couplings: accounting for correlations between motions and alignment. *J. Am. Chem. Soc.*, **125**, 10530–10531.

37. Al-Hashimi,H.M., Tolman,J.R., Majumdar,A., Gorin,A. and Patel,D.J. (2001) Determining stoichiometry in homomultimeric nucleic acid complexes using magnetic field induced residual dipolar couplings. *J. Am. Chem. Soc.*, **123**, 5806–5807.

38. Weis,W.I. and Dickamer,K. (1996) Structural basis of lectin-carbohydrate recognition. *Annu. Rev. Biochem.*, **65**, 441–473.

39. Hermann,T. and Westhof,E. (1999) Docking of cationic antibiotics to negatively charged pockets in RNA folds. *J. Med. Chem.*, **42**, 1250–1261.

40. Davis,B., Afshar,M., Varani,G., Murchie,A.I.H., Karn,J., Lentzen,G., Drysdale,M., Bower,J., Potter,A.J., Starkey,I.D. *et al.* (2004) Rational design of inhibitors of HIV-1 TAR RNA through the stabilisation of electrostatic 'hot spots'. *J. Mol. Biol.*, **336**, 343–356.

41. Athanassiou,Z., Dias,R.L.A., Moehle,K., Dobson,N., Varani,G. and Robinson,J.A. (2004) Structural mimicry of retroviral Tat proteins by constrained, beta-hairpin peptidomimetics: Ligands with high affinity and selectivity for viral TAR RNA regulatory elements. *J. Am. Chem. Soc.*, **126**, 6906–6913.

42. Aboulela,F., Karn,J. and Varani,G. (1995) The structure of the human-immunodeficiency-virus type-1 TAR RNA reveals principles of RNA recognition by Tat protein. *J. Mol. Biol.*, **253**, 313–332.

43. Jaeger,J.A. and Tinoco,I. (1993) An NMR-study of the HIV-1 TAR element hairpin. *Biochemistry*, **32**, 12522–12530.

44. Colvin,R.A., White,S.W., Garciablanco,M.A. and Hoffman,D.W. (1993) Structural features of an RNA containing the CUGGGA loop of the human-immunodeficiency-virus type-1 transactivation response element. *Biochemistry*, **32**, 1105–1112.

45. Kulinski,T., Olejniczak,M., Huthoff,H., Bielecki,L., Pachulska-Wieczorek,K., Das,A.T., Berkhout,B. and Adamiak,R.W. (2003) The apical loop of the HIV-1 TAR RNA hairpin is stabilized by a cross-loop base pair. *J. Biol. Chem.*, **278**, 38892–38901.

46. Huq,I. and Rana,T.M. (1997) Probing the proximity of the core domain of an HIV-1 Tat fragment in a Tat-TAR complex by affinity cleaving. *Biochemistry*, **36**, 12592–12599.